Bioorganic & Medicinal Chemistry 17 (2009) 195–202

Contents lists available at ScienceDirect

Bioorganic & Medicinal Chemistry

journal homepage: www.elsevier.com/locate/bmc

Identification of trimannoside-recognizing peptide sequences from a T7 phage display screen using a QCM device

Kazusa Nishiyama [a], Yoichi Takakusagi [b], Tomoe Kusayanagi [b], Yuki Matsumoto [b], Shiori Habu [b], Kouji Kuramochi [b], Fumio Sugawara [b], Kengo Sakaguchi [b], Hideyo Takahashi [c], Hideaki Natsugari [c], Susumu Kobayashi [a,*]

[a] Department of Medicinal and Life Science, Faculty of Pharmaceutical Sciences, Tokyo University of Science, 2641 Yamazaki, Noda, Chiba 278-8510, Japan
[b] Department of Applied Biological Science, Faculty of Science and Technology, Tokyo University of Science, 2641 Yamazaki, Noda, Chiba 278-8510, Japan
[c] Laboratory of Synthetic Organic and Medicinal Chemistry, School of Pharmaceutical Sciences, Teikyo University, Sagamiko, Sagamihara, Kanagawa 229-0195, Japan

ARTICLE INFO

Article history:
Received 1 October 2008
Revised 4 November 2008
Accepted 4 November 2008
Available online 8 November 2008

Keywords:
T7 phage display
QCM
Self-assembled monolayer (SAM)
Trimannose
Polysaccharide
Peptide

ABSTRACT

Here, we report on the identification of trimannoside-recognizing peptide sequences from a T7 phage display screen using a quartz-crystal microbalance (QCM) device. A trimannoside derivative that can form a self-assembled monolayer (SAM) was synthesized and used for immobilization on the gold electrode surface of a QCM sensor chip. After six sets of one-cycle affinity selection, T7 phage particles displaying PSVGLFTH (8-mer) and SVGLGLGFSTVNCF (14-mer) were found to be enriched at a rate of 17/44, 9/44, respectively, suggesting that these peptides specifically recognize trimannoside. Binding checks using the respective single T7 phage and synthetic peptide also confirmed the specific binding of these sequences to the trimannoside-SAM. Subsequent analysis revealed that these sequences correspond to part of the primary amino acid sequence found in many mannose- or hexose-related proteins. Taken together, these results demonstrate the effectiveness of our T7 phage display environment for affinity selection of binding peptides. We anticipate this screening result will also be extremely useful in the development of inhibitors or drug delivery systems targeting polysaccharides as well as further investigations into the function of carbohydrates in vivo.

1. Introduction

The biological role of sugar chains in higher organisms has been intensively studied over a number of decades. Recent research has revealed insights into the biological role of polysaccharides with regard to the cell–cell interaction,[1] pathogen invasion,[2] serum stability of the proteins,[3,4] and the mechanism of quality control of glycoproteins in the endoplasmic reticulum (ER).[5,6] Recent advances in glycoprotein research have also revealed that changes in the glycosylation pattern of cellular glycoproteins are common features of human cancer.[1] Indeed, such changes can influence tumor progression, suggesting that an inhibitor of glycosylation may slow down the development of certain types of cancer.[7]

There have been significant advances in the development of oligosaccharide libraries generated by chemical synthesis together with efficient methods of isolating natural glycoproteins.[8–11] These developments have facilitated studies with regard to the biological role of polysaccharides. Among them, the mechanism of quality control of glycoproteins in ER has been gradually clarified over the past decade. Glycosylation of the nascent polypeptide and subsequent processing of the non-reducing end of the polysaccharide chain by glycosidases and glycosyltransferases define the fate of the glycoprotein,[12,13] which is cooperatively supported by the function of polysaccharide-recognizing proteins called lectins. Various molecular chaperones, cargo receptors and ubiquitin ligases contribute to maintaining the fidelity of glycoprotein synthesis in the ER.[5,10,14–18] In this mechanism, triglucosyl high-mannose type oligosaccharide ($Glc_3Man_9GlcNAc_2$, G3M9) is a common precursor of the *N*-glycans (Fig. 1).[5,10] This oligosaccharide comprises a trimannosyl core anchored by two *N*-acetylglucosamine (GlcNAc) units for the asparagine (Asn) residue in the Asn-X-Ser/Thr motif of the nascent polypeptide chain. At the opposite side of non-reducing end are three branches, designated D1, D2, and D3 arms, composed of glucose and mannose units (Fig. 1). The residues in these chains are trimmed by glycosidases during the early stages of the biosynthetic pathway and transmitted as a reporter for ER lectin-chaperones, such as calreticulin (CRT) and calnexin (CNX).[5,19]

Identification of the (poly)saccharide-recognizing primary peptide sequences would be an approach to investigate the precise mode of binding of carbohydrate-related proteins, including lectins.[20,21] This information may also facilitate the discovery of new species of proteins using a similarity search as well as generating peptides that can selectively target the polysaccharide chain

* Corresponding author. Tel.: +81 4 7124 1501x6543.
E-mail address: kobayash@rs.noda.tus.ac.jp (S. Kobayashi).

0968-0896/$ - see front matter © 2008 Elsevier Ltd. All rights reserved.
doi:10.1016/j.bmc.2008.11.004

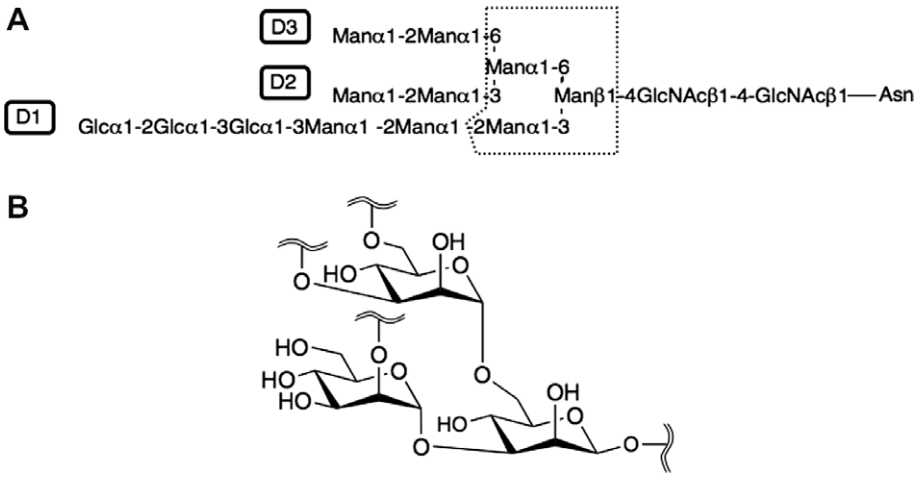

Figure 1. (A) Structure of triglucosyl high-mannose type oligosaccharide ($Glc_3Man_9GlcNAc_2$, G3M9). Trimannosyl core is shown boxed. (B) Chemical structure of the trimannosyl core.

for drug delivery or inhibit the corresponding function. Herein, we attempted to identify peptide sequences that can specifically recognize trimannoside, the core structure in *N*-glycans as a scaffold for branches D1–3 (Fig. 1B). A pea lectin, concanavalin A, is known to specifically recognize this skeleton in many complex glycans. Indeed, the mode of docking is well defined by X-ray crystallography.[22–24] In order to identify the binding-peptide sequence, we used the T7 phage display technology.[25,26] Recently, we have reported the T7 phage display screen combined with the cuvette type quartz-crystal microbalance (QCM) biosensor, which enables rapid and efficient identification of binding proteins or peptides for small organic molecules of interest.[27,28] The target immobilization process on the gold electrode surface of the sensor chip involves a self-assembled monolayer (SAM). Importantly, SAM acts as a superior scaffold for the QCM biosensor by accumulating the substrate of interest on the gold surface, thereby increasing the sensitivity of the frequency changes.[29] Thus, after synthesizing a trimannoside derivative that can form SAM, we performed an affinity selection using a HepG2-derived T7 phage pool. Herein, we describe the experimental details, biological significance of the resulting peptides and the effectiveness of our T7 phage display environment for affinity selection of binding peptides.

2. Results and discussion

2.1. Synthesis of trimannoside derivative

A trimannoside derivative (**14**) that forms SAM on the gold electrode was synthesized as shown in Scheme 1. The trimannoside was synthesized according to the previous report,[30,31] and then connected with a tetraethyleneglycol unit that can reduce nonspecific binding of T7 phages.[29] This product was finally coupled with compound **12**, which facilitates chemisorption of the molecule of interest onto the gold electrode surface via thiol–Au interactions. Accumulation of the trimannoside on the gold electrode is brought about by alignment of the C11 alkyl chains.[29]

2.2. Affinity selection of trimannoside-recognizing peptides using a HepG2-derived T7 phage pool

The trimannoside derivative (**14**) was dissolved in 75% ethanol, dropped onto the gold electrode and then incubated for 16 h under a humid and shaded atmosphere at room temperature (rt), which resulted in the formation of trimannoside-SAM on the gold electrode surface. After washing the surface of the electrode, the sensor chip was placed in the QCM apparatus using a buffer filled cuvette. The QCM sensor was then fully stabilized. When an aliquot of plaque forming units (pfu) of a HepG2-derived T7 phage pool was injected into the cuvette, a frequency change was detected (Fig. 2). After monitoring the interaction for 10 min, the sensor chip was detached from the device. The genomic DNA of trimannoside-recognizing phage on the gold electrode surface was then recovered using the host *Escherichia coli* (BLT5615) solution and amplified. After 30 min incubation at 37 °C, recovered phage particles were arbitrarily extracted from the resulting T7 phage solution and the enrichment was analyzed by sequencing the DNA encoding the fusion protein of the phage capsid. Peptide sequences obtained after six sets of individual one-cycle screens are summarized in Table 1. Forty-four phage particles were arbitrarily extracted from the resulting T7 phage solution and the enrichment was analyzed by sequencing the DNA encoding the fusion protein of the phage capsid. The T7 phage display screen using trimannoside-SAM and QCM resulted in enrichment of T7 phages whose capsid fusion peptides corresponded to PSVGLFTH (8-mer) and SVGLGLGFSTVNCF (14-mer), which were included at a rate of 17 and 9 out of 44 phage isolates, respectively (Table 1).

2.3. Binding experiment using the respective single T7 phage and synthetic peptide on a QCM apparatus

In order to characterize the interaction with trimannoside, T7 phage particles displaying PSVGLFTH (phage 1) or SVGLGLG FSTVNCF (phage 2) was amplified by infection of host cells and used for binding experiments. According to the same procedure of screening, an aliquot of 10^{10} pfu/ml of each single phage pool was individually injected into the cuvette and the frequency change monitored for 10 min.[27] Figure 3 shows the relative binding of each phage to trimannoside as calculated from the frequency decrease 10 min after injection. The frequency change obtained with control T7 phage (NSPAGISRELVDKLAAALE) is also shown as a reference. Phages 1 and 2, which were both significantly enriched in the screen, showed an interaction with trimannoside, verifying the result of the selection. Similarly, synthetic peptide that corresponds to each sequence showed a binding to free trimannose, confirming the specific interaction between the two molecules (Fig. 4). The dissociation constant is predicted to be at the order of 10^{-4} M or more because 200 μM of trimannose was needed to obtain the minimal response on QCM. However, because of low

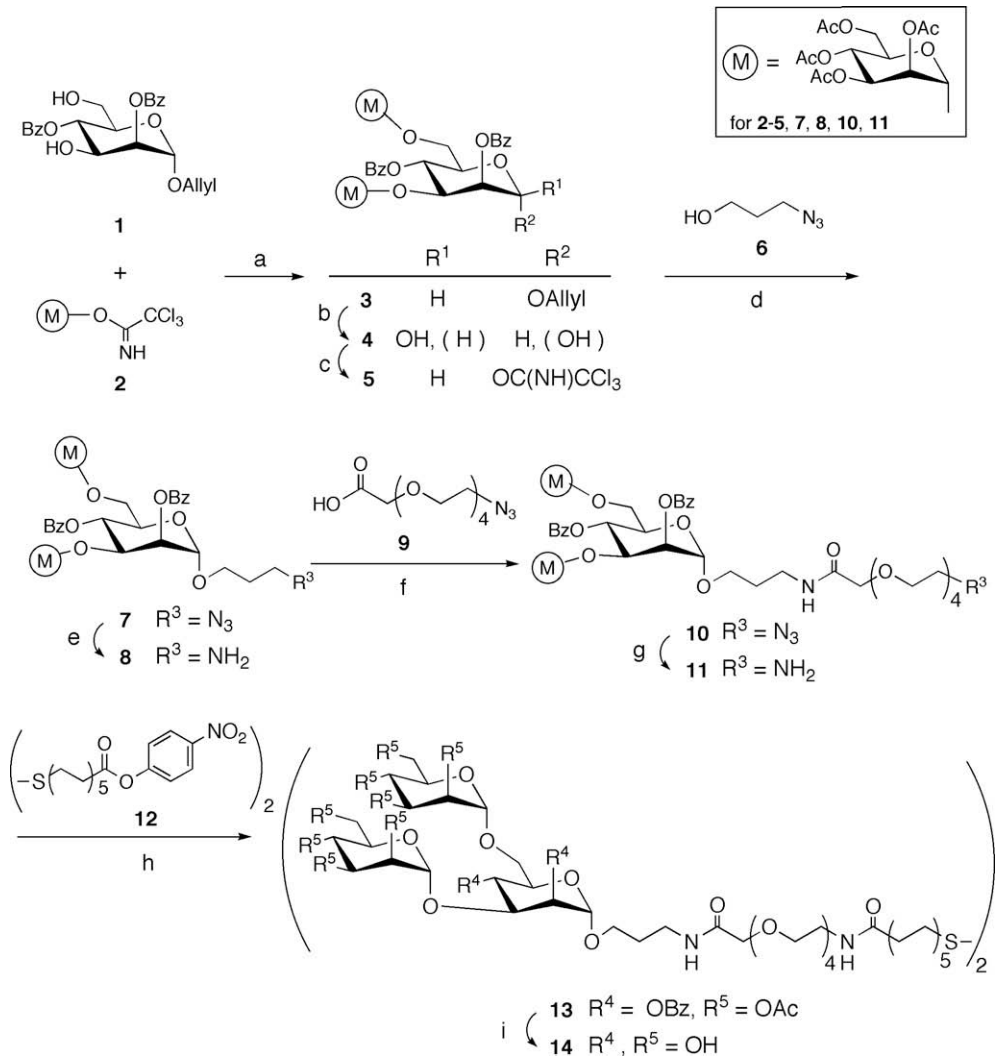

Scheme 1. Synthesis of trimannoside derivative (**14**). Reagents and conditions: (a) TMSOTf, CH_2Cl_2, 0 °C, 72%; (b) $Pd(PPh_3)_4$, AcOH, 80 °C, 74%; (c) CCl_3CN, DBU, CH_2Cl_2, rt, 84%; (d) TMSOTf, CH_2Cl_2, 0 °C, 72%; (e) $Pd(OH)_2/C$, H_2, EtOH–THF, rt; (f) WSCI, HOBt, DIPEA, CH_2Cl_2, rt, 86% (two steps); (g) $Pd(OH)_2/C$, H_2, EtOH–THF, rt, 88%; (h) WSCI, HOBt, DIPEA, CH_2Cl_2, rt, 59% (i) NaOMe, MeOH, rt, 87%.

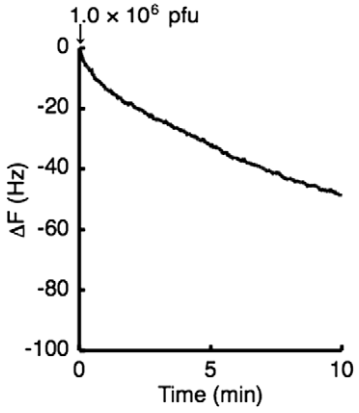

Figure 2. A representative QCM sensorgram obtained by an affinity selection of peptide on the QCM apparatus (AffinixQ) using the trimannoside derivative and a HepG2 cell-derived T7 phage pool (8 μl). The trimannoside-immobilized ceramic sensor chip generated by SAM was first attached to the QCM apparatus. After injecting the T7 phage pool at the indicated concentration, the frequency decrease was monitored for 10 min.

Table 1
Trimannoside-SAM-selected peptide sequence and enrichment ratio after six sets of individual one-cycle screens

Phage number	Peptide sequence on phage capsid	Ratio
1	PSVGLFTH	17/44
2	SVGLGLGFSTVNCF	9/44

solubility of the synthetic peptides or requirement of a considerable amount of trimannose, accurate kinetic constant could not be determined. Nevertheless, these experiments confirmed that each peptide can selectively recognize trimannoside.

2.4. Biological significance of trimannoside-recognizing peptide sequences

Even though we used a T7 phage pool with mRNA derived from HepG2 cells for the trimannoside-SAM screen, no phage that fully matched lectins or enzymes were identified. We reasoned that there must be many proteins that are not displayed on the T7

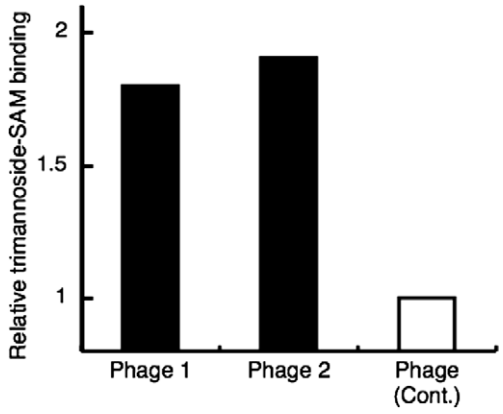

Figure 3. Relative binding of single phage clones to trimannoside-SAM. An aliquot of 10^7 pfu/ml (final) of respective phage pool was injected into the cuvette and the frequency changes were monitored for 10 min. The size of each frequency change is compared with that using control phage (white bar) and shown as a black bar. Phage 1: PSVGLFTH (8-mer), phage 2: SVGLGLGFSTVNCF (14-mer), phage (cont.): NSPAGISRELVDKLAAALE (19-mer).

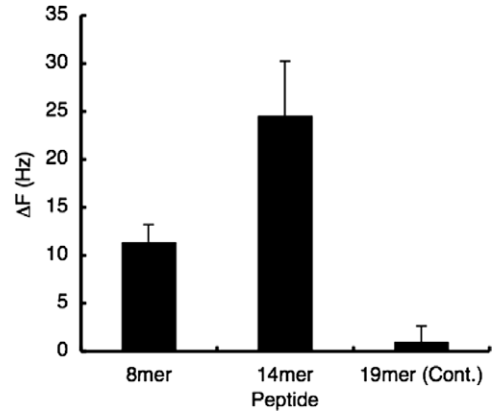

Figure 4. Binding analysis between trimannose and immobilized synthetic peptide. Trimannose (final concentration 200 μM) was added to the cuvette. Interaction with synthetic peptide immobilized on a gold electrode of a ceramic sensor chip was then monitored until the frequency change reaches equilibrium. $N = 3$; data represented as means ± SE.

phage capsid or selected in the screen because of problems associated with misfolding, low solubility or abundance. Nonetheless, the binding experiment clearly demonstrated the interaction between trimannoside and the obtained phages displaying short peptides (Fig. 3). Thus, based on the available chemical and biological information concerning the polysaccharides, we dissected the significance of the obtained peptide sequences.

A similarity search of human proteins using PSVGLFTH or SVGLGLGFSTVNCF as a query sequence against the SwissProt database identified approximately 500 potential hits. Tables 2 and 3 summarizes the carbohydrate-related proteins ranked by PSI-BLAST. In addition to mannose-related enzymes (bold in Tables 2 and 3), other hexose-related enzymes or lectins are included in this list (plain), suggesting that the primary sequence corresponding to the affinity-selected peptides may be important for recognition of the hexose skeleton (Suppl. Tables 1 and 2). Furthermore, a series of E3 ubiquitin ligases in the ubiquitin–proteasome pathway, which are involved in the degradation of misfolded *N*-glycans in the ER,[16,17] were also identified as candidate hits in this similarity search. Thus, the partial sequence identified in this screen may be a common feature of proteins that recognize the *N*-glycan component of glycoproteins. The information obtained in this study will be useful in further investigations regarding the biochemistry of carbohydrates in vivo, including analysis of the quality control process of glycoproteins in the ER.

3. Conclusion

In the present study, we synthesized a trimannoside derivative that forms SAM and performed a T7 phage display screen using a QCM device. As a result of an affinity selection using a HepG2-derived T7 phage pool we identified two peptides, PSVGLFTH (8-mer) and SVGLGLGFSTVNCF (14-mer), as candidate trimannoside-recognition sequences. A similarity search using these peptide sequences suggested that they correspond to part of the primary sequence of carbohydrate-related proteins. We believe that this preliminary examination will contribute to a better understanding of the interaction between (poly)saccharides and these protein mediators. Furthermore, these peptide sequences may be a useful starting point for generating inhibitors that target molecules involved in cancer progression. In conclusion, we have demonstrated the effectiveness of the T7 phage display environment and obtained crucial information regarding trimannoside-protein interactions.

4. Experimental

4.1. Instruments

A 27-MHz QCM device, AffinixQ and ceramic sensor chip was purchased from Initium Inc. (Tokyo, Japan). PCR was performed using a PTC-200 (Peltier Thermal Cycler) (BIO-RAD, Hercules, CA). Sequencing analysis was carried out using an ABI PRISM 3100 Genetic Analyzer (Applied Biosystems, Foster City, CA). Centrifugation was performed using a MX-201 centrifuge (TOMY Industry, Tokyo, Japan).

4.2. General (chemistry)

All non-aqueous reactions were carried out using freshly distilled solvents under an atmosphere of argon. All reactions were monitored by TLC, which was carried out on Silica Gel 60 F254 plates (E. Merck, Darmstadt, Germany). Flash chromatography separations were performed on BW820 (Fuji Silysia Co., Ltd, Kasugai, Japan).

The NMR spectra (^{1}H, ^{13}C) were determined on a Bruker 600 MHz or 400 MHz spectrometer (Avance DRX-600, Avance DRX-400) or a JEOL 400 MHz spectrometer (JNM-LD400), using $CDCl_3$ (with TMS for ^{1}H NMR and chloroform-*d* for ^{13}C NMR as the internal reference) solution, unless otherwise noted. Chemical shifts were expressed in parts per million (ppm) and coupling constants are in Hertz. Optical rotations were recorded using $CHCl_3$ as a solvent of a JASCO P-1030 digital polarimeter at rt, using the sodium D line. Infrared spectra (IR) were recorded on a Jasco FT/IR-410 spectrometer using NaCl (neat) or KBr pellets (solid), and reported as wavenumbers (cm^{-1}). Mass spectra (MS) were obtained on LCMS-IT-TOF (Shimazu, Kyoto, Japan). Sodium trifluoroacetate (TFA–Na) was used as internal standard for high resolution MS.

4.3. Synthesis of trimannoside-SAM compound

4.3.1. Allyl 2,3,4,6-tetra-*O*-acetyl-α-D-mannopyranosyl-(1 → 3)-[2,3,4,6-tetra-*O*-acetyl-α-D-mannopyranosyl-(1 → 6)]-2,4-di-*O*-benzoyl-α-D-mannopyranoside (3)

TMSOTf (0.03 mmol) was added to a mixture of **1**[30,31] (248 mg, 0.58 mmol), 2,3,4,6-tetra-*O*-acetyl-α-D-mannopyranosyl-2,2,2-trichloroacetimidate **2** (857 mg, 1.74 mmol) and 4 Å molecular sieves in anhydrous CH_2Cl_2 (8 ml) at 0 °C under an Ar atmosphere. The

Table 2
Summary of human carbohydrate-related protein that contain a sequence resembling PSVGLFTH

No.	Score	Protein name [Homo sapiens]
1	**19.3**	**Endoplasmic reticulum mannosyl-oligosaccharide 1,2-alpha-mannosidase**
2	17.6	Inositol-trisphosphate 3-kinase B
3	**16.8**	**GPI mannosyltransferase 4**
4	16.8	E3 ubiquitin–protein ligase HUWE1
5	16.8	Sialidase-3 (Membrane sialidase)
6	16.8	Galactosylgalactosylxylosylprotein 3-beta-glucuronosyltransferase 3
7	**15.5**	**Sugar phosphate exchanger 2**
8	15.5	UDP-glucuronosyltransferase 3A2 precursor
9	15.5	Thioesterase superfamily member 5
10	15.5	E3 ubiquitin–protein ligase HECTD1
11	15.5	*N*-Acetyl-beta-glucosaminyl-glycoprotein 4-beta-*N*-acetylgalactosaminyltransferase 2 (NGalNAc-T2)
12	15.5	UDP-glucuronosyltransferase 3A1 precursor
13	15.5	Lipopolysaccharide-binding protein precursor (LBP)
14	15.5	Phosphatidylinositol *N*-acetylglucosaminyltransferase subunit H
15	**15.5**	**Protein *O*-mannosyl transferase 2**
16	15.5	Dolichol phosphate-mannose biosynthesis regulatory protein
17	**15.5**	**Sugar phosphate exchanger 3**
18	15.5	Platelet glycoprotein 4
19	15.1	6-phosphofructokinase, muscle type
20	14.6	Ubiquitin-conjugating enzyme E2 O (Ubiquitin–protein ligase O)
21	**14.6**	**Glycoprotein *endo*-alpha-1,2-mannosidase-like protein**
22	**14.6**	**Glycoprotein *endo*-alpha-1,2-mannosidase (Mandaselin)**
23	14.6	Phosphatidylinositol 3,4,5-trisphosphate-dependent Rac exchanger 1 protein (P-Rex1)
24	14.6	Phosphatidylinositol-glycan-specific phospholipase D precursor (PI-G PLD)
25	14.6	Probable E3 ubiquitin–protein ligase HERC2

Table 3
Summary of human carbohydrate-related protein that contains a sequence resembling SVGLGLGFSTVNCF

No.	Score	Protein name [Homo sapiens]
1	19.7	Glycosyltransferase 54 domain-containing protein precursor
2	**19.3**	**Glucose-1,6-bisphosphate synthase**
3	19.3	Ubiquitin–protein ligase E3C
4	18.0	Ubiquitin carboxyl-terminal hydrolase 24 (ubiquitin thioesterase 24)
5	**18.0**	**Lysosomal alpha-mannosidase precursor**
6	**18.0**	**Alpha-1,6-mannosylglycoprotein 6-beta-*N*-acetylglucosaminyltransferase B**
7	18.0	Globoside alpha-1,3-*N*-acetylgalactosaminyltransferase 1
8	17.6	Beta-1,3-galactosyl-*O*-glycosyl-glycoprotein beta-1,6-*N*-acetylglucosaminyltransferase 7
9	17.6	Probable *O*-sialoglycoprotein endopeptidase 2
10	17.6	E3 ubiquitin–protein ligase RNF19A
11	17.6	Fructose-1,6-bisphosphatase 1 (FBPase 1)
12	**17.6**	**Hexokinase-3**
13	17.2	Probable E3 ubiquitin–protein ligase HERC2
14	17.2	Probable E3 ubiquitin–protein ligase MYCBP2
15	17.2	Glucose-6-phosphate translocase (glucose-5-phosphate transporter)
16	16.8	Beta-galactosidase-1-like protein 3
17	16.8	Chondroitin sulfate synthase 1
18	16.8	Phosphatidylinositol 4-kinase type 2-beta
19	16.8	1-phosphatidylinositol-4,5-bisphosphate phosphodiesterase beta-4
20	**16.8**	**Mannose-P-dolichol utilization defect 1 protein (Suppressor of Lec15 and Lec35 glycosylation mutation homolog) (SL15)**
21	16.8	Chondroitin sulfate synthase 2
22	16.8	Trehalase precursor
23	16.8	Sialic acid-binding Ig-like lectin 11 precursor
24	16.3	Fructosamine-3-kinase

mixture was stirred for 1 h, and then neutralized with saturated aqueous $NaHCO_3$. The mixture was extracted with CH_2Cl_2, and the organic phase was dried, filtered, and concentrated in vacuo. The residue was purified by silica gel chromatography (hexane/EtOAc = 1:1) to yield **3** (452 mg, 72%). $[\alpha]_D^{27}$ +22.56 (c = 0.25 in $CHCl_3$); ^{1}H NMR (600 MHz, $CDCl_3$) δ 8.14 (2H, m), 8.04 (2H, m), 7.54 (6H, m), 5.97 (1H, m), 5.62 (1H, t, J = 10.2 Hz), 5.52 (1H, dd, J = 3.6 Hz, 1.8 Hz), 5.41 (1H, m), 5.36 (1H, m), 5.31 (1H, m), 5.25 (1H, m), 5.23 (1H, dd, J = 4.8 Hz, 1.8 Hz), 5.62 (3H, m), 4.99 (1H, d, 1.8 Hz), 4.88 (1H, dd, J = 4.8 Hz, 1.8 Hz), 4.80 (1H, d, J = 1.2 Hz), 4.51 (1H, dd, J = 10.2 Hz, 3.6 Hz), 4.16 (5H, m) 4.07 (1H, m), 4.03 (1H, dd, J = 13.8 Hz, 1.8 Hz), 3.99 (1H, dd, J = 14.4 Hz, 2.4 Hz), 3.91 (1H, dd, J = 10.8 Hz, 7.2 Hz), 3.60 (1H, dd, J = 10.8 Hz, 2.4 Hz), 2.12 (3H, s), 2.11 (3H, s), 2.05 (3H, s), 1.98 (3H, s), 1.94 (3H, s), 1.93 (3H, s), 1.86 (3H, s), 1.83 (3H, s); ^{13}C NMR (150 MHz, $CDCl_3$) δ 171.1, 170.6, 170.5, 169.9, 169.7, 169.6, 169.5, 169.1, 169.0, 165.9, 165.3, 133.6, 133.5, 132.9, 129.9, 129.8, 129.1, 128.7, 128.5, 118.7, 99.4, 97.0, 96.2, 75.4, 71.8, 69.5, 69.3, 69.2, 68.9, 68.7, 68.6, 68.5, 68.2, 66.6, 65.9, 65.8, 62.2, 62.1, 60.3, 20.8, 20.6, 20.6, 20.6, 20.5, 20.5, 20.4, 20.4; IR (neat) 3024, 2955, 1755, 1603, 1452, 1372, 1232, 1047, 978, 937, 756, 715 cm^{-1}; HRMS (ESI) calcd for $C_{51}H_{60}O_{26}$ $[M+Na]^+$: 1111.3271, found 1111.3242.

4.3.2. 2,3,4,6-tetra-*O*-acetyl-α-D-mannopyranosyl-(1 → 3)-[2,3,4,6-tetra-*O*-acetyl-α-D-mannopyranosyl-(1 → 6)]-2,4-di-*O*-benzoyl-α-D-mannopyranose (4)

To a solution of **3** (286 mg, 0.26 mmol) in anhydrous AcOH (2.6 ml) was added $Pd(PPh_3)_4$ (91 mg, 0.08 mmol) at rt. The mix-

ture was stirred for 1 h at 80 °C. Toluene was added and then the solvents were evaporated in vacuo to give a residue, which was purified by silica gel column chromatography (hexane/EtOAc = 1:2) to give **4** (205 mg, 74%). $[\alpha]_D^{24}$ −7.61 (*c* = 1.0 in $CHCl_3$); ^{1}H NMR (600 MHz, $CDCl_3$) δ 8.14 (2H, m), 8.04 (2H, m), 7.58 (4H, m), 7.45 (2H, m), 5.58 (1H, t, *J* = 10.2 Hz), 5.54 (1H, dd, *J* = 3.6 Hz, 1.8 Hz), 5.45 (1H, m), 5.36 (1H, dd, *J* = 10.2 Hz, 3.6 Hz), 5.23 (1H, t, *J* = 10.2 Hz), 5.20 (1H, dd, *J* = 3.6 Hz, 1.8 Hz), 5.10 (2H, m), 4.99 (1H, d, *J* = 1.8 Hz), 4.89 (1H, m), 4.81 (1H, d, *J* = 1.8 Hz), 4.57 (1H, dd, *J* = 10.2 Hz, 3.6 Hz), 4.38 (1H, m), 4.21 (1H, dd, *J* = 12.0 Hz, 5.4 Hz), 4.10 (4H, m), 3.99 (1H, dd, *J* = 12.0 Hz, 1.8 Hz), 3.89 (1H, dd, *J* = 10.8 Hz, 7.2 Hz), 3.66 (1H, dd, *J* = 10.8 Hz, 1.8 Hz), 2.13 (3H, s), 2.12 (3H, s), 2.05 (3H, s), 1.99 (3H, s), 1.98 (3H, s), 1.94 (3H, s), 1.86 (3H, s), 1.83 (3H, s); ^{13}C NMR (150 MHz, $CDCl_3$) δ 171.2, 170.1, 170.1, 170.0, 169.9, 169.8, 169.1, 169.1, 165.9, 165.4, 133.6, 133.6, 130.0, 130.0, 128.7, 128.6, 128.6, 128.5, 99.4, 97.4, 92.2, 74.7, 72.1, 69.6, 69.4, 69.3, 69.2, 69.1, 68.5, 68.4, 66.3, 66.1, 62.4, 62.3, 60.4, 60.4, 21.1, 20.9, 20.8, 20.7, 20.7, 20.6, 20.5, 20.4; IR (neat) 3470, 3026, 2941, 1745, 1603, 1452, 1371, 1226, 1047, 756, 716 cm^{-1}; HRMS (ESI) calcd for $C_{48}H_{56}O_{26}$ $[M+Na]^+$: 1071.2958, found 1071.2938.

4.3.3. 2,3,4,6-tetra-*O*-acetyl-α-D-mannopyranosyl-(1 → 3)-[2,3,4,6-tetra-*O*-acetyl-α-D-mannopyranosyl-(1 → 6)]-2,4-di-*O*-benzoyl-α-D-mannopyranosyl trichloroacetimidate (5)

To a stirred solution of **4** (325 mg, 0.31 mmol) in anhydrous CH_2Cl_2 (3 ml) was added trichloroacetonitrile (12.5 μl, 1.24 mmol) and DBU (8.8 μl, 0.06 mmol) at 0 °C. The mixture was stirred for 1 h at rt. The solvents were removed in vacuo. The residue was purified by silica gel column chromatography (hexane/EtOAc = 1:1 to 1:2) to give **5** (308 mg, 83%). ^{1}H NMR (600 MHz, $CDCl_3$) δ 8.95 (1H, s), 8.17 (2H, m), 8.05 (2H, m), 7.61 (4H, m), 7.47 (2H, m), 6.47 (1H, d, *J* = 1.8 Hz), 5.45 (1H, t, *J* = 9.6 Hz), 5.67 (1H, dd, *J* = 3.6 Hz, 1.8 Hz), 5.29 (1H, dd, *J* = 10.2 Hz, 3.6 Hz), 5.25 (1H, t, *J* = 10.2 Hz), 5.20 (1H, dd, *J* = 3.6 Hz, 1.8 Hz), 5.15 (1H, t, *J* = 9.6 Hz), 5.11 (1H, dd, *J* = 9.6 Hz, 3.6 Hz), 5.07 (1H, d, *J* = 1.8 Hz), 4.91 (1H, dd, *J* = 3.0 Hz, 2.4 Hz), 4.78 (1H, d, 1.8 Hz), 4.53 (1H, dd, *J* = 9.6 Hz, 3.6 Hz), 4.32 (1H, m), 4.18 (2H, m), 4.07 (2H, m), 3.96 (1H, dd, *J* = 12.0 Hz, 1.8 Hz), 3.94 (1H, dd, *J* = 12.0 Hz, 2.4 Hz), 3.90 (1H, dd, *J* = 11.4 Hz, 6.6 Hz), 3.67 (1H, dd, *J* = 11.4 Hz, 1.8 Hz), 2.11 (3H, s), 2.08 (3H, s), 2.06 (3H, s), 1.98 (3H, s), 1.95 (3H, s), 1.92 (3H, s), 1.89 (3H, s), 1.84 (3H, s); ^{13}C NMR (150 MHz, $CDCl_3$) δ 170.6, 170.5, 169.9, 169.7, 169.6, 169.5, 169.2, 169.1, 165.7, 165.2, 159.6, 133.9, 133.7, 130.2, 129.9, 129.0, 128.9, 128.7, 128.6, 128.5, 128.5, 128.2, 99.7, 97.2, 94.3, 75.6, 72.0, 70.3, 69.4, 69.2, 68.9, 68.4, 68.2, 68.0, 67.9, 66.3, 65.9, 65.7, 62.2, 61.9, 53.4, 20.8, 20.7, 20.6, 20.6, 20.6, 20.5; HRMS (ESI) calcd for $C_{50}H_{56}O_{26}NCl_3$ $[M+Na]^+$: 1214.2054, found 1214.2053.

4.3.4. 3-Azidopropyl-2,3,4,6-tetra-*O*-acetyl-α-D-mannopyranosyl-(1 → 3)-[2,3,4,6-tetra-*O*-acetyl-α-D-mannopyranosyl-(1 → 6)]-2,4-di-*O*-benzoyl-α-D-mannopyranoside (7)

A solution of 3-azido-1-propanol **6**[32,33] (173 mg, 1.71 mmol) and **5** (227 mg, 0.19 mmol) in dry CH_2Cl_2 (2 ml), containing 4 Å molecular sieves, was stirred under Ar at 0 °C. Then TMSOTf (2.8 μl, 0.015 mmol) was added, and the reaction mixture was stirred for 1 h. The mixture was neutralized with aqueous $NaHCO_3$. The organic layer was dried, filtered, and concentrated. The residue was purified by column chromatography (hexane/EtOAc = 1:1) to obtain **7** (155 mg, 72%). $[\alpha]_D^{26}$ +12.48 (*c* = 0.5 in $CHCl_3$); ^{1}H NMR (600 MHz, $CDCl_3$) δ 8.14 (2H, m), 8.04 (2H, m), 7.61 (2H, m), 7.54 (2H, m), 7.47 (2H, m), 5.59 (1H, t, *J* = 10.2 Hz), 5.50 (1H, dd, *J* = 3.6 Hz, 1.8 Hz), 5.34 (1H, dd, *J* = 10.2 Hz, 3.6 Hz), 5.24 (1H, t, *J* = 10.2 Hz), 5.22 (1H, dd, *J* = 3.6 Hz, 1.8 Hz), 5.11 (2H, m), 5.04 (1H, d, *J* = 1.8 Hz), 5.02 (1H, d, *J* = 1.8 Hz), 4.88 (1H, m), 4.80 (1H, d, *J* = 1.8 Hz), 4.44 (1H, dd, *J* = 10.2 Hz, 3.6 Hz), 4.08 (8H, m), 3.95 (1H, dd, *J* = 10.2 Hz, 2.4 Hz), 3.91 (2H, m), 3.63 (1H, m), 3.59 (1H, dd, *J* = 10.8 Hz, 1.8 Hz), 3.49 (2H, m), 2.12 (3H, s), 2.11 (3H, s), 2.05 (3H, s), 1.98 (3H, s), 1.94 (3H, s), 1.91 (3H, s), 1.88 (3H, s), 1.83 (3H, s); ^{13}C NMR (150 MHz, $CDCl_3$) δ 170.6, 170.5, 170.2, 169.9, 169.7, 169.6, 169.2, 168.9, 165.9, 165.4, 133.7, 133.6, 129.9, 129.9, 129.0, 128.8, 128.7, 128.5, 99.6, 97.4, 97.0, 75.9, 71.8, 69.7, 69.4, 69.3, 69.2, 68.9, 68.6, 68.3, 66.4, 65.9, 65.8, 65.2, 62.3, 62.1, 60.6, 48.3, 28.8, 20.8, 20.8, 20.7, 20.6, 20.6, 20.5, 20.5; IR (neat) 2939, 2100, 1749, 1603, 1452, 1371, 1226, 1047, 756, 715 cm^{-1}; HRMS (ESI) calcd for $C_{51}H_{61}O_{26}N_3$ $[M+Na]^+$: 1154.3441, found 1154.3429.

4.3.5. Azide derivative 10

The mixture of azide **7** (266 mg, 0.24 mmol) and Pd on C (130 mg) in THF/EtOH (1:1) was stirred under hydrogen atmosphere at rt for 50 min. The catalyst was filtered off, and the filtrate was condensed in vacuo to give a crude preparation of **8** as syrup. The crude **8** and 14-azido-3,6,9,12-tetraoxatetradecanoic acid **9**[29] (0.71 mmol, 195 mg) was dissolved in dry CH_2Cl_2 (3 ml) at rt. Then, WSCI–HCl (90 mg, 0.47 mmol), DIPEA (130 μl, 0.71 mmol), and HOBt (0.47 mmol, 64 mg) was added to the mixture. After 12 h, the mixture was diluted with CH_2Cl_2, washed with H_2O, and the organic layer was dried, filtered, and concentrated in vacuo. The crude residue was purified by silica gel chromatography (CH_2Cl_2/MeOH = 9:1) to obtain **10** (294 mg, 90%, two steps yield from **7**). $[\alpha]_D^{21}$ = +6.36 (*c* = 1.0 in $CHCl_3$); ^{1}H NMR (600 MHz, $CDCl_3$) δ 8.15 (2H, m), 8.07 (2H, m), 7.63 (1H, m), 7.59 (1H, m), 7.55 (2H, m), 7.46 (2H, m), 7.12 (1H, br m), 5.66 (1H, t, *J* = 9.6 Hz), 5.49 (1H, dd, *J* = 3.0 Hz, 1.8 Hz), 5.34 (1H, dd, *J* = 10.2 Hz, 3.6 Hz), 5.24 (2H, m), 5.10 (2H, m), 5.03 (1H, d, *J* = 1.8 Hz), 5.02 (1H, d, *J* = 1.8 Hz), 4.87 (1H, dd, *J* = 3.0 Hz, 1.8 Hz), 4.80 (1H, d, *J* = 1.8 Hz), 4.46 (1H, dd, *J* = 9.6 Hz, 3.0 Hz), 4.09 (3H, m), 4.02 (5H, m), 3.96 (1H, m), 3.90 (1H, m), 3.85 (1H, m), 3.69 (15H, m), 3.58 (2H, m), 3.48 (1H, m), 3.38 (4H, m), 2.11 (3H, s), 2.10 (3H, s), 2.06 (3H, s), 1.98 (3H, s), 1.92 (3H, s), 1.90 (3H, s), 1.88 (3H, s), 1.82 (3H, s); ^{13}C NMR (150 MHz, $CDCl_3$) δ 170.6, 170.5, 169.9, 169.9, 169.8, 169.7, 169.6, 169.2, 169.0, 165.9, 165.3, 133.6, 133.5, 129.9, 129.1, 128.8, 128.7, 128.5, 99.5, 97.4, 97.1, 76.1, 71.8, 70.9, 70.6, 70.5, 70.2, 70.0, 70.0, 69.4, 69.4, 69.3, 69.2, 68.9, 68.5, 68.4, 68.3, 66.4, 66.0, 65.9, 65.8, 62.3, 62.1, 53.4, 50.6, 35.9, 29.5, 20.8, 20.7, 20.7, 20.6, 20.6, 20.6, 20.5, 20.4; IR (neat) 3385, 2934, 2878, 2100, 1739, 1672, 1602, 1539, 1452, 1371, 1226, 1043, 979, 756, 715 cm^{-1}; HRMS (ESI) calcd for $C_{61}H_{80}O_{31}N_4$ $[M+Na]^+$: 1387.4704, found 1387.4701.

4.3.6. Protected trimannoside derivative (13)

The mixture of **10** (200 mg, 0.15 mmol) and Pd on C (100 mg) in THF/EtOH (1:1) was stirred was stirred under hydrogen atmosphere at rt for 60 min. The catalyst was filtered off, and the filtrate was condensed in vacuo to give **11** as syrup. A mixture of **11** (172 mg) and **12**[29] (0.04 mmol, 30 mg) in dry THF (4 ml) was stirred at rt for 12 h. Then the mixture was concentrated, and the residue was purified by silica gel chromatography to yield **13** (78.2 mg, 52%, two steps yield). $[\alpha]_D^{21}$ +6.61 (*c* = 1.25 in $CHCl_3$); ^{1}H NMR (600 MHz, $CDCl_3$) δ 8.14 (2H × 2, m), 8.07 (2H × 2, m), 7.60 (2H × 2, m), 7.55 (2H × 2, m), 7.46 (2H × 2, m), 7.11 (1H × 2, br m), 6.19 (1H × 2, br m), 5.65 (1H × 2, t, *J* = 9.6 Hz), 5.49 (1H × 2, dd, *J* = 3.0 Hz, 1.8 Hz), 5.34 (1H × 2, dd, *J* = 10.2 Hz, 3.6 Hz), 5.24 (2H × 2, m), 5.10 (2H × 2, m), 5.03 (1H × 2, d, *J* = 1.8 Hz), 5.02 (1H × 2, d, *J* = 1.8 Hz), 4.87 (1H × 2, dd, *J* = 3.0 Hz, 1.8 Hz), 4.80 (1H × 2, d, *J* = 1.8 Hz), 4.46 (1H × 2, dd, *J* = 9.6 Hz, 3.0 Hz), 4.14 (3H × 2, m), 4.02 (5H × 2, m), 3.96 (1H × 2, dd, *J* = 12.0 Hz, 2.4 Hz), 3.90 (1H × 2, dd, *J* = 10.8 Hz, 6.6 Hz), 3.85 (1H × 2, m), 3.68 (8H × 2, m), 3.63 (5H × 2, m), 3.58 (2H × 2, m), 3.55 (2H × 2, m), 3.49 (1H × 2, m), 3.42 (2H × 2, m), 2.67 (2H × 2, t, *J* = 7.2 Hz), 2.12 (2H × 2, t, *J* = 7.2 Hz), 2.11 (3H × 2, s), 2.10

(3H × 2, s), 2.06 (3H × 2, s), 1.98 (3H × 2, s), 1.95 (2H × 2, m), 1.92 (3H × 2, s), 1.89 (3H × 2, s), 1.88 (3H × 2, s), 1.82 (3H × 2, s), 1.66 (2H × 2, m), 1.62 (2H × 2, m), 1.37 (2H × 2, m), 1.27 (10H × 2, br s); ^{13}C NMR (150 MHz, $CDCl_3$) δ 173.2 (×2), 170.5 (×2), 170.5 (×2), 169.9 (×2), 169.8 (×2), 169.7 (×2), 169.6 (×2), 169.2 (×2), 169.0 (×2), 165.9 (×2), 165.3 (×2), 133.6 (×2), 133.5 (×2), 130.0 (×2), 129.9 (× 2), 129.1 (×2), 128.8 (×2), 128.5 (×2), 99.5 (×2) 97.4 (×2), 97.0 (×2), 76.1 (×2), 71.8 (×2), 70.8 (×2), 70.6 (× 2), 70.5 (×2), 70.4 (×2), 70.4 (×2), 70.3 (×2), 70.1 (×2), 69.9 (×2), 69.4 (×2), 69.3 (×2), 69.3 (×2), 69.2 (×2), 69.0 (×2), 68.6 (×2), 68.4 (×2), 68.3 (×2), 66.4 (×2), 66.0 (×2), 65.9 (×2), 65.8 (×2), 62.3 (×2), 62.1 (×2), 39.1 (×2), 36.6 (×2), 35.9 (×2), 29.4 (×2), 29.4 (×2), 29.4 (×2), 29.3 (×2), 29.3 (×2), 29.2 (×2), 29.2 (×2), 29.2 (×2), 28.5 (×2), 25.7 (×2), 20.8 (×2), 20.7 (×2), 20.6 (×2), 20.6 (×2), 20.5 (×2), 20.5 (×2), 20.4 (×2), 20.4 (×2); IR (neat) 2928, 2363, 1751, 1655, 1543, 1256, 1371, 1228, 1091, 1051, 756, 713 cm^{-1}; HRMS (ESI) calcd for $C_{144}H_{202}O_{64}N_4S_2$ $[M+Na]^+$: 3098.2023, found 3098.2014.

4.3.7. Trimannoside derivative (14)

A mixture of **13** (45 mg, 0.015 mmol) and NaOMe (4 mg, 0.07 mmol) in MeOH (1.5 ml) was stirred at rt for 2 days. Then the mixture was concentrated, and the residue was purified by reverse phase silica gel chromatography (H_2O/MeOH = 1:4 to 1:1) to yield trimannoside derivative **14** (26 mg, 87%). $[\alpha]_D^{27}$ +38.1 (c = 0.1 in $CHCl_3$); ^{1}H NMR (600 MHz, $CDCl_3$) δ 5.08 (1H × 2, d, J = 1.2 Hz), 4.83 (1H × 2, d, J = 1.2 Hz), 4.69 (1H × 2, d, J = 1.2 Hz), 4.03 (2H × 2, s), 3.98 (1H × 2, dd, J = 3.6 Hz, 1.8 Hz), 3.90 (1H × 2, dd, J = 10.8 Hz, 6.0 Hz), 3.86 (1H × 2, dd, J = 3.6 Hz, 1.8 Hz), 3.80 (5H × 2, m), 3.74 (4H × 2, m), 3.66 (15H × 2, m), 3.56 (2H × 2, t, J = 5.4 Hz), 3.46 (1H × 2, m), 3.41 (2H × 2, m), 3.34 (2H × 2, m), 2.67 (2H × 2, t, J = 7.2 Hz), 2.19 (2H × 2, t, J = 7.8 Hz), 1.82 (2H × 2, m), 1.67 (2H × 2, m), 1.59 (2H × 2, br m), 1.39 (2H × 2, br m), 1.31 (10H × 2, br s); ^{13}C NMR (150 MHz, $CDCl_3$) δ 176.4 (×2), 172.7 (×2), 103.9 (×2), 101.9 (×2), 101.4 (×2), 80.8 (×2), 74.9 (×2), 74.4 (×2), 74.1 (×2), 73.5 (×2), 72.6 (×2), 72.5 (×2), 72.1 (×2), 72.1 (×2), 72.0 (×2), 71.6 (×2), 71.5 (×2), 71.4 (×2), 71.4 (×2), 71.3 (×2), 71.2 (×2), 70.6 (×2), 68.8 (×2), 68.6 (×2), 67.5 (×2), 67.3 (×2), 66.5 (×2), 62.9 (×2), 40.3 (×2), 39.8 (×2), 37.4 (×2), 37.1 (×2), 30.8 (×2), 30.6 (×2), 30.6 (×2), 30.4 (×2), 30.4 (×2), 30.3 (×2), 30.3 (×2), 30.2 (×2), 29.4 (×2), 27.0 (×2); IR (neat) 3358, 2924, 2855, 1653, 1458, 1101 cm^{-1}; HRMS (ESI) calcd for $C_{84}H_{154}O_{44}N_4S_2$ $[M+Na]^+$: 1985.9299, found 1985.9318.

4.4. Construction of a T7 phage pool

A T7 phage pool was constructed using HepG2 cell-derived cDNA according to the previous reports.[29] The primary titer of this T7 phage pool was 5.0×10^6 pfu/ml. For the screening procedure, the phage pool was amplified up to 1.28×10^8 pfu/ml using *E. coli* (BLT5615) as the host strain.

4.5. Procedure for the T7 phage display screen using a cuvette type QCM apparatus

A 20 μl aliquot of trimannoside derivative (**14**) (1 mM in 75% EtOH) was dropped onto the gold electrode of the ceramic sensor chip and left for 16 h under a humid and shaded atmosphere at rt. The surface of the electrode was washed for 10 min in buffer (10 mM Tris–HCl, pH 8.0, 200 mM NaCl), which was stirred at 1000 rpm. The sensor chip was setup for the QCM apparatus with the cuvette containing 8 ml of buffer. The QCM sensor was then allowed to fully stabilize. An aliquot of 8 μl of T7 phage pool (1.28×10^8 pfu/ml) was then injected into the cuvette. Frequency changes, caused by binding to the trimannoside immobilized on the gold electrode surface were then monitored for 10 min. For the recovery of bound phages, 10 μl of host *E. coli* (BLT5615) solution (cultured for 30 min at 37 °C in the presence of 1 mM of IPTG beforehand) was dropped onto the gold electrode and then incubated at 37 °C for 30 min. To the resulting solution was then added another 200 μl of LB medium. An aliquot of phage was then extracted from this solution and subjected to PCR analysis followed by agarose gel electrophoresis and DNA sequencing.

4.6. Agarose gel electrophoresis and DNA sequencing

Agarose gel electrophoresis and DNA sequencing were performed as described previously.[29]

4.7. Preparation of peptide

The proposed trimannside-recognizing peptide PSVGLFTH (8-mer), SVGLGLGFSTVNCF (14-mer) or the control peptide NSPAGISRELVDKLAAALE (19-mer) was synthesized by the Fmoc method using a peptide synthesizer PS-3 (Aloka, Tokyo, Japan).[28] By using Fmoc-Gly-Wang-resin (0.61 mmol/g, Carbiochem, San Diego, CA) and adding 0.4 mmol of each amino acid (Carbiochem) sequentially, the peptide chain (PSVGLFTH, SVGLGLGFSTVNCF or NSPAGISRELVDKLAAALE) was extended from the C terminal to the N terminal end by repeating the process of Fmoc deprotection using 20% piperidine in DMF (6 ml), activation by HBTU (0.4 mmol) and 0.4 M 4-methylmorpholine in DMF (3 ml), and amino acid coupling with the resin. The resultant material was treated with 4 ml of cleavage cocktail (0.75 g phenol, 0.25 ml 1,2-ethanedithiol, 0.5 ml thioanisole in 10 ml of 95% TFA) for 3 h to cleave the peptide from the resin and deprotect the side chains. After cold ether precipitation, the precipitant was washed with ether three times and recovered for HPLC purification.

4.8. Peptide purification

The peptide was purified using a reverse phase preparative HPLC instrument (SSC-3461, Senshu Scientific, Tokyo, Japan) equipped with a CAPCELL PAK C-18 column (ϕ20 × 250 mm, UG 120 Å, Shiseido, Tokyo, Japan) that was kept at 40 °C.[28] A binary gradient with a flow rate of 4 ml/min was employed; A phase: 0.05% TFA aq, B phase: 0.05% TFA in MeOH. The gradient condition was as follows; PSVGLFTH: 5% B (0 min)–100% B (20 min)–100% B (30 min), SVGLGLGFSTVNCF: 80% B (0 min) –80% B (30 min), NSPAGISRELVDKLAAALE: 65% B (0 min)–85% B (30 min). The UV absorption at 210 or 280 nm was monitored using a UV detector (SSC-5200, Senshu Scientific). The peaks detected at 22 min (PSVGLFTH), 16 min (SVGLGLGFSTVNCF) and 28 min (NSPAGISRELVDKLAAALE) under each gradient condition were fractionated and dried up to obtain the purified peptides. The identity of the peptide was verified by ESI-IT-MS [Esquire 3000 Plus, Bruker Daltonics, Billerica, MA].

4.9. Kinetic analysis by QCM

The synthetic peptide was immobilized on gold electrode surface of a sensor chip [NSPSVGLFTH: 193 Hz (5.2 pmol), SVGLGLGFSTVNCF: 243 Hz (5.0 pmol), NSPAGISRELVDKLAAALE: 542 Hz (8.1 pmol)]. After immersing the sensor chip in 8 ml of saline solution (200 mM NaCl in 10 mM Tris–HCl, pH 8.0), 8 μl of trimannose (200 mM) were added in buffer at 25 °C and monitored until the frequency change reaches equilibrium.

4.10. Bioinformatics tool

We searched for human proteins containing identical or similar sequences to the peptides identified from the phage screening pro-

cedure, NSPSVGLFTH (8-mer) or SVGLGLGFSTVNCF (14-mer), using the Position-Specific Iterated Basic Local Alignment Search Tool (PSI-BLAST, NCBI) (http://www.ncbi.nlm.nih.gov/blast/Blast.cgi) and the SwissProt database.

Acknowledgments

This work was partially supported by a Grant-in-Aid for Scientific Research (The Ministry of Education, Culture, Sports, Science and Technology of Japan, Japan Society for the Promotion of Science).

Supplementary data

Supplementary data associated with this article can be found, in the online version, at doi:10.1016/j.bmc.2008.11.004.

References and notes

1. Zhao, Y. Y.; Takahashi, M.; Gu, J. G.; Miyoshi, E.; Matsumoto, A.; Kitazume, S.; Taniguchi, N. *Cancer Sci.* **2008**, *99*, 1304.
2. van Kooyk, Y.; Geijtenbeek, T. B. *Nat. Rev. Immunol.* **2003**, *3*, 697.
3. Christensen, D.; Foged, C.; Rosenkrands, I.; Nielsen, H. M.; Andersen, P.; Agger, E. M. *Biochim. Biophys. Acta* **2007**, *1768*, 2120.
4. Christensen, D.; Kirby, D.; Foged, C.; Agger, E. M.; Andersen, P.; Perrie, Y.; Nielsen, H. M. *Biochim. Biophys. Acta* **2008**, *1778*, 1365.
5. Kamiya, Y.; Kato, K. *Trend. Glycosci. Glycotech.* **2006**, *18*, 231.
6. Ito, Y.; Hagihara, S.; Matsuo, I.; Totani, K. *Curr. Opin. Struct. Biol.* **2005**, *15*, 481.
7. Fiaux, H.; Kuntz, D. A.; Hoffman, D.; Janzer, R. C.; Gerber-Lemaire, S.; Rose, D. R.; Juillerat-Jeanneret, L. *Bioorg. Med. Chem.* **2008**, *16*, 7337.
8. Suda, Y.; Arano, A.; Fukui, Y.; Koshida, S.; Wakao, M.; Nishimura, T.; Kusumoto, S.; Sobel, M. *Bioconjug. Chem.* **2006**, *17*, 1125.
9. Hanashima, S.; Inamori, K.; Manabe, S.; Taniguchi, N.; Ito, Y. *Chemistry* **2006**, *12*, 3449.
10. Hagihara, S.; Goda, K.; Matsuo, I.; Ito, Y. *Biochem. Biophys. Res. Commun.* **2007**, *360*, 357.
11. Ito, Y.; Hagihara, S.; Arai, M. A.; Matsuo, I.; Takatani, M. *Glycoconjug. J.* **2004**, *21*, 257.
12. Totani, K.; Ihara, Y.; Matsuo, I.; Koshino, H.; Ito, Y. *Angew. Chem. Int. Ed. Engl.* **2005**, *44*, 7950.
13. Totani, K.; Ihara, Y.; Matsuo, I.; Ito, Y. *J. Biol. Chem.* **2006**, *281*, 31502.
14. Yamaguchi, D.; Kawasaki, N.; Matsuo, I.; Totani, K.; Tozawa, H.; Matsumoto, N.; Ito, Y.; Yamamoto, K. *Glycobiology* **2007**, *17*, 1061.
15. Kamiya, Y.; Kamiya, D.; Yamamoto, K.; Nyfeler, B.; Hauri, H. P.; Kato, K. *J. Biol. Chem.* **2008**, *283*, 1857.
16. Yoshida, Y.; Chiba, T.; Tokunaga, F.; Kawasaki, H.; Iwai, K.; Suzuki, T.; Ito, Y.; Matsuoka, K.; Yoshida, M.; Tanaka, K.; Tai, T. *Nature* **2002**, *418*, 438.
17. Mizushima, T.; Hirao, T.; Yoshida, Y.; Lee, S. J.; Chiba, T.; Iwai, K.; Yamaguchi, Y.; Kato, K.; Tsukihara, T.; Tanaka, K. *Nat. Struct. Mol. Biol.* **2004**, *11*, 365.
18. Kamiya, Y.; Yamaguchi, Y.; Takahashi, N.; Arata, Y.; Kasai, K.; Ihara, Y.; Matsuo, I.; Ito, Y.; Yamamoto, K.; Kato, K. *J. Biol. Chem.* **2005**, *280*, 37178.
19. Tatami, A.; Hon, Y. S.; Matsuo, I.; Takatani, M.; Koshino, H.; Ito, Y. *Biochem. Biophys. Res. Commun.* **2007**, *364*, 332.
20. Matsubara, T.; Ishikawa, D.; Taki, T.; Okahata, Y.; Sato, T. *FEBS Lett.* **1999**, *456*, 253.
21. Ishikawa, D.; Kikkawa, H.; Ogino, K.; Hirabayashi, Y.; Oku, N.; Taki, T. *FEBS Lett.* **1998**, *441*, 20.
22. Rini, J. M.; Hardman, K. D.; Einspahr, H.; Suddath, F. L.; Carver, J. P. *J. Biol. Chem.* **1993**, *268*, 10126.
23. Naismith, J. H.; Field, R. A. *J. Biol. Chem.* **1996**, *271*, 972.
24. Loris, R.; Maes, D.; Poortmans, F.; Wyns, L.; Bouckaert, J. *J. Biol. Chem.* **1996**, *271*, 30614.
25. Smith, G. P. *Science* **1985**, *228*, 1315.
26. Smith, G. P.; Petrenko, V. A. *Chem. Rev.* **1997**, *97*, 391.
27. Takakusagi, Y.; Takakusagi, K.; Kuramochi, K.; Kobayashi, S.; Sugawara, F.; Sakaguchi, K. *Bioorg. Med. Chem.* **2007**, *15*, 7590.
28. Takakusagi, Y.; Kuroiwa, Y.; Sugawara, F.; Sakaguchi, K. *Bioorg. Med. Chem.* **2008**, *16*, 7410.
29. Takakusagi, Y.; Kuramochi, K.; Takagi, M.; Kusayanagi, T.; Manita, D.; Ozawa, H.; Iwakiri, K.; Takakusagi, K.; Miyano, Y.; Nakazaki, A.; Kobayashi, S.; Sugawara, F.; Sakaguchi, K. *Bioorg. Med. Chem.* **2008**, *16*, 9837.
30. Du, Y.; Zhang, M.; Kong, F. *Org. Lett.* **2000**, *2*, 3797.
31. Du, Y.; Zhang, M.; Kong, F. *Tetrahedron* **2001**, *57*, 1757.
32. Pearson, W. H.; Bergmeier, S. C.; Chytra, J. A. *Synthesis* **1990**, 156.
33. Lefeber, D. J.; Kamerling, J. P.; Vliegenthart, J. F. *Chemistry* **2001**, *7*, 4411.